

COMPREHENSIVE ELECTRO-MAGNETIC, THERMAL, AND STRUCTURAL FINITE ELEMENT ANALYSIS OF THE LITHIUM COLLECTION LENS AT THE FNAL ANTIPROTON SOURCE*

P. Hurh[#], J. Morgan, S.Tariq, FNAL, Batavia, IL 60510, USA

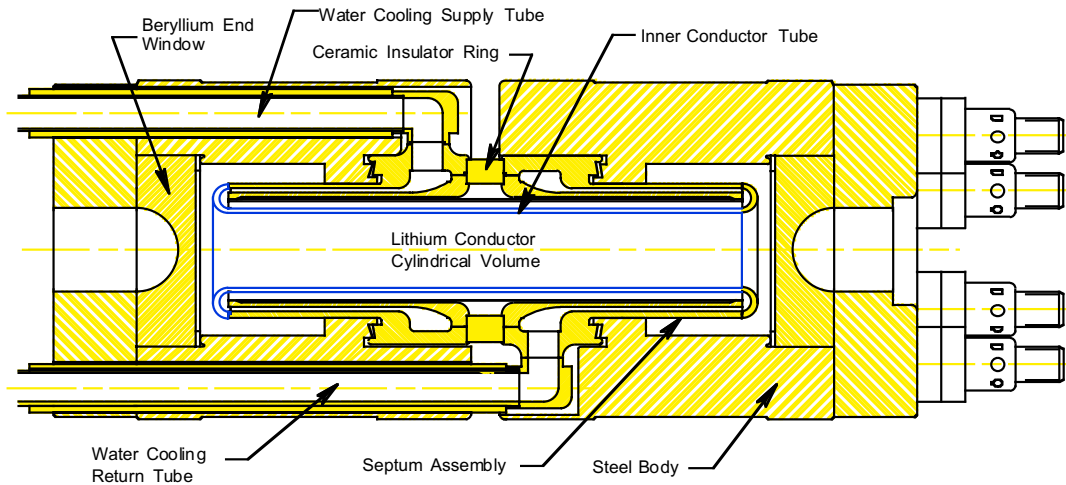


Figure 1: Cross-section diagram of Collection Lens Device. Septum conductor tube is shown in blue.

Abstract

A history of lithium Collection Lens failures at lower than designed focusing strengths has led to extensive efforts to quantify the Lens loading environment and structural behavior. A comprehensive finite element analysis (FEA) model of the lithium Lens has been developed as part of these efforts and as a tool to aid in future lithium lens design improvements. The FEA model includes complete device geometry, the excitement current pulse (damped sine wave), temperature dependent electrical, thermal and structural (including strain rate dependent) material properties. Latest results, including transient electro-magnetic, thermal and structural solutions, for the currently operational lithium Lens design are presented.

INTRODUCTION

The FNAL Antiproton Source incorporates a lithium Collection Lens to greatly improve the transmission efficiency of antiprotons into the Debuncher ring. The Lens has a large axial current passing through a solid lithium cylinder that produces a strong magnet field proportional to the radius. The design gradient of the 1 cm radius Lens was 1,000 T/m (10 Tesla surface field). However, operational lenses have not been able to sustain the design gradient for enough pulses to be practical, usually failing within days or weeks due to mechanical failures of the titanium tube that contains the lithium, historically called the septum [1]. Running Lenses at

reduced gradient has allowed them to survive for an acceptable length of time, millions of pulses. The penalty for lowering the gradient is less antiproton yield due to reduced focusing strength. The operational gradient of the Collection Lens is 745 T/m.

The cross-section of the Lens device is shown in Figure 1. The most stressed part of the septum is the conductor tube. Stresses arise from several loading sources such as thermal expansion from ohmic and beam heating, magnetic forces from the current pulse, and structural loading from clamping bolts and lithium filling pre-load. In order to gain insight into the loading environment and structural behavior of the Lens, a comprehensive FEA model has been created.

MODEL DESCRIPTION

Using ANSYS® [2] FEA software a 10 degree wedge-shaped half model of the functional elements of the Lens was created to simulate the magnetic response of the Lens to a damped sine wave current pulse (angular freq. of 8622 Hz and damping coefficient of 1500 Hz). Joule heating results from this model were then applied to a matching thermal model of the Lens along with beam heating loads (estimated from MARS target simulations), transformer heating loads (estimated from empirical measurements), and cooling loads (estimated from ANSYS® FLOTTRAN analysis). Temperature results from the thermal model were then read back into the magnetic model in order to re-evaluate material properties at the new temperature distribution. Each current pulse was broken into 10 steps (37 μ sec each) with a cooling period of 2 seconds between pulses.

*Work supported by the US Department of Energy under contract No. DE-AC02-76CH03000.

[#]hurh@fnal.gov

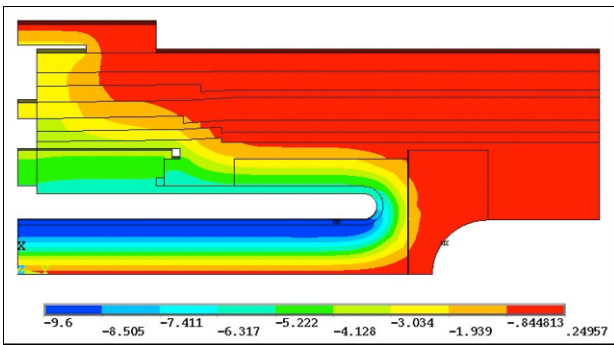


Fig. 2: B θ (Tesla) for H.G. pulse at time of beam passage.

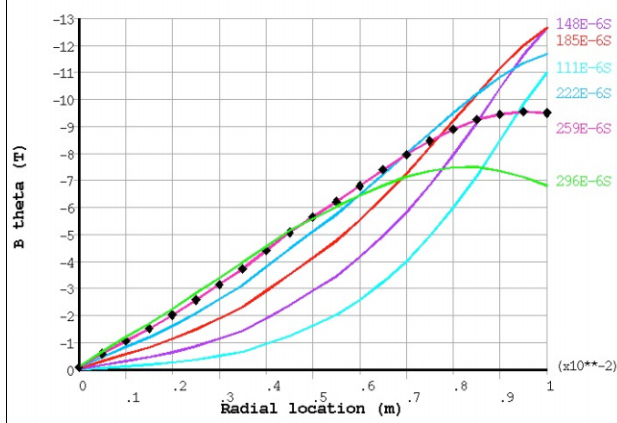


Fig. 3: B θ vs Radius for various times. Dots denote time of beam passage.

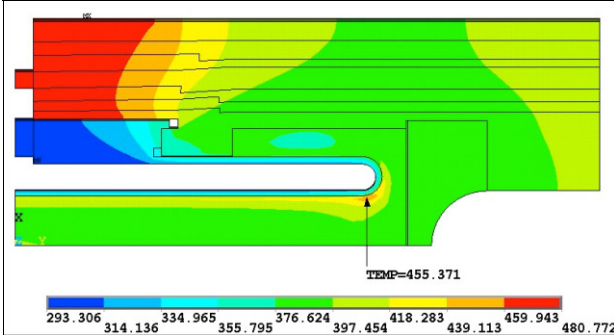


Fig. 4: Temp distribution. just after 400th H.G. pulse (K).

Nodal forces and temperature distributions were then applied to a matching structural model along with additional structural loads from the lithium pre-load and the tie-rod clamping forces.

As can be seen from the following results, the behavior of the lithium is essential to understanding the load environment. Lithium is a structurally soft material that exhibits viscoplastic hardening as well as creep softening. Results from viscoplastic tensile testing [3] were incorporated in this analysis, but as of this writing, creep effects have not yet been incorporated.

Three loading scenarios were simulated. First, a benchmark simulation was run to compare calculated temperature results with measured results. Second, a simulation was run with low gradient (L.G.) parameters (745 T/m, 500 kA peak current, 5E12 protons on target, 2

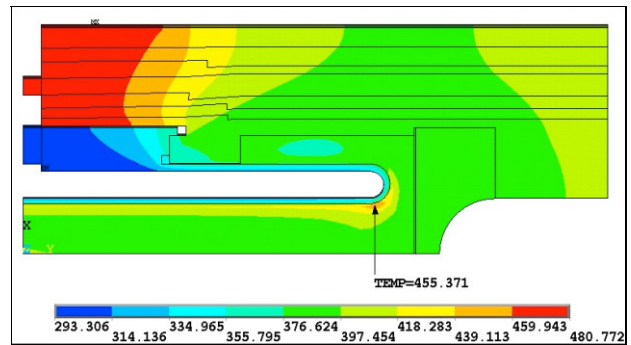


Fig. 5: Temp dist. just before 401st H.G. pulse (K).

sec pulse repetition period). Finally a third simulation was run with the same parameters as the second, but with a high gradient (H.G.) pulse (1,000 T/m, 670 kA).

RESULTS

For the sake of brevity most of the results pictured in the figures will be for the H.G. simulation. Comparisons to the lower gradient simulations will be made in the text.

Magnetic results of the model are as expected. The magnetic flux density in the theta direction is shown in Figure 2 for the time of beam passage. Figure 3 shows how the magnetic flux density changes with radius and time.

Figure 4 shows the temperature distribution in the Lens just after the 400th high gradient pulse. The hottest spot in the lithium is 182.4 °C. This is significant since the melting point of lithium is 180.6 °C. In comparison the lithium hot spot at the lower gradient is 120.6 °C. Figure 5 shows the temperature distribution just before the 401st high gradient pulse. Note that the hottest temperatures in the Lens are in the steel body half which is not directly cooled by water.

Although not pictured here, it is worth noting that the benchmark simulation results indicated temperatures in an instrumented area of the body half of 80 to 85 °C. This agrees with measured temperatures of 77 to 82 °C.

Figure 6 shows a vector plot of the displacement of the lithium during the peak magnetic forces of a high gradient pulse. It shows how the radially inward forces push the lithium out of the ends of the septum conductor tube. In addition, a small amount of lithium near the opening of the tube is shown to be moving back into the void created by the inwardly moving lithium. This indicates separation of the lithium from the septum tube wall is probable.

This possibility is further confirmed by looking at the hoop stress in the conductor tube versus time in Figure 7. The dip into negative stress when magnetic forces are the highest indicates that the tube is going into compression. Ideally, if the lithium pre-load is adequate, the tube wall should only be exposed to tensile stresses to avoid stress reversals. After the Lens warms up to quasi-static conditions, this lithium/titanium separation effect decreases in severity since the effective pre-load is increased by thermal expansion of the lithium. Figure 8 shows the hoop stress in the conductor tube for later high

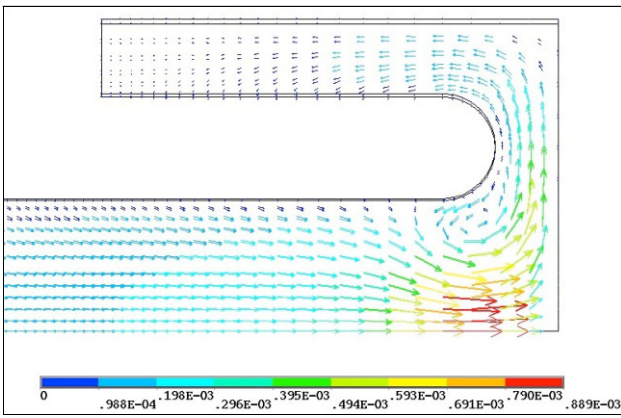


Fig. 6: Lithium displacement (m) at peak of H.G. pulse.

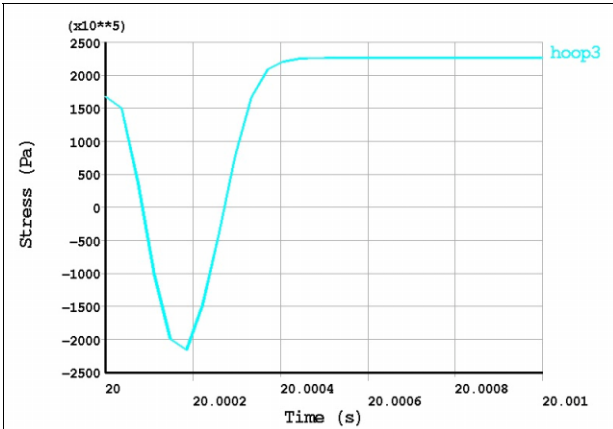


Fig. 7: Conductor tube hoop stress (Pa) in 1st H.G. pulse.

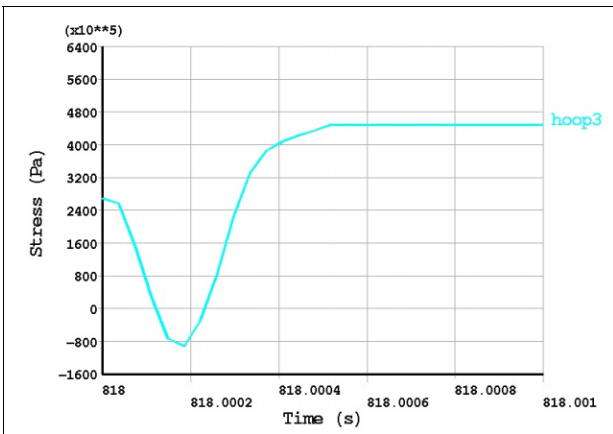


Fig. 8: Cond. tube hoop stress (Pa) in 400th H.G. pulse.

gradient pulses and can be compared to the curve in Figure 9 for the low gradient simulation.

Figure 10 shows the hoop stress in the conductor tube at points of maximum extremes during a quasi-static high gradient pulse. Displacements have been exaggerated by a factor of 20.

CONCLUSION

Although far from complete, this analysis has already yielded some significant results. There are obvious signs that at higher gradient, portions of the lithium may become liquid. Adding cooling to the body could help since a significant amount of heat is originating there.

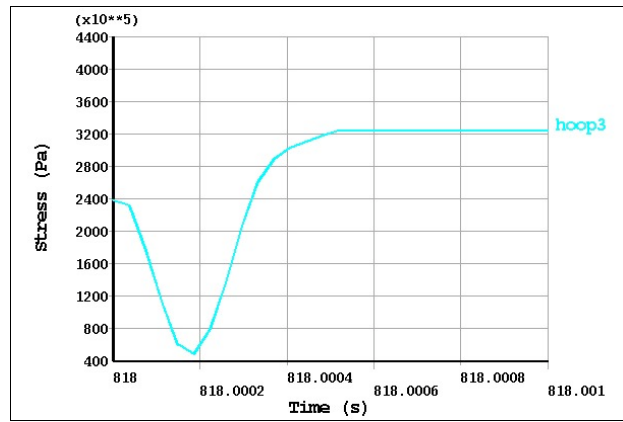


Fig. 9: Cond. tube hoop stress (Pa) in 400th L.G. pulse.

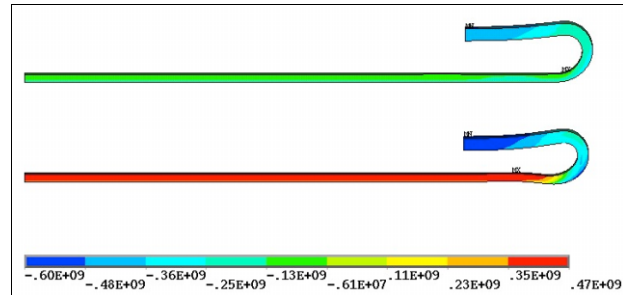


Fig. 10: Conductor tube hoop stress extremes (Pa) for 400th H.G. pulse at peak magnetic forces (top) and peak lithium temperature (bottom).

There are indications that at higher gradient the lithium may be separating from the septum conductor tube and causing detrimental stress reversals in the tube wall. Elimination of the buffer regions and/or higher lithium pre-loads may help avoid this effect. At higher gradient the estimated loading cycle (470 MPa, R=-.2) is nearing or surpassing fatigue thresholds for the Ti 6Al-4V alloy (462 MPa, R=.1, gentle surface grind [4]).

Future work should incorporate creep effects since significant recovery of plastic deformation between pulses could significantly alter the stress distribution in the septum tube. In addition, the high strains in the lithium suggest that lithium failure may be occurring. The behavior of failed lithium in compression is a complicated and probably unquantifiable phenomena. Future studies should be undertaken to ensure that the lithium failure limit in compression is not being surpassed.

REFERENCES

- [1] P. Hurh, "Examination Results of Failed Collection Lens Septa 20 and 21", Fermilab MSDNote #MSDN-ME-000022 (2002).
- [2] ANSYS® is a registered trademark of SAS IP Inc.
- [3] S. Tariq, K. Ammigan, P. Hurh, R. Schultz, P. Liu, & J. K. Shang, "Li Material Testing- Fermilab Antiproton Source Lithium Collection Lens", TPAG013, PAC 2003, Portland (2003).
- [4] Titanium and Titanium Alloys: Source Book, M. J. Donachie, Jr. Ed., American Society for Metals, Metals Park, p. 355 (1982).